Qiong Wu, Xisong Miao*, Hai Wang, Yongmei Wu, Jun Li, Jing Lu, Qingyan Zhou and Hongping Ju*

Supramolecular architecture based on high-lacunary sandwich-type building blocks: synthesis, characterization, and properties

DOI 10.1515/znb-2015-0202
Received December 1, 2015; accepted February 18, 2016

Abstract: The new supramolecular compound $[Fe_2(AsMo_7O_{27})_2](H_2en)_2(NH_4)_8{\cdot}6H_2O$ (**1**) (en = ethylenediamine) has been synthesized in aqueous solution and characterized by elemental analysis, thermal analysis, and single crystal X-ray diffraction. The structural analysis has revealed that **1** represents the first example of a polyoxometalate-based sandwich-type supramolecular hybrid constructed from hexalacunary building blocks. Owing to the presence of ethylenediammonium cations, the $[Fe_2(AsMo_7O_{27})_2]^{12-}$ units are stabilized by multiple circular hydrogen bonds extending the structure into a 2D supramolecular framework. The magnetic properties and antitumor activities of **1** have also been studied.

Keywords: antitumor activity; polyoxometalate; sandwich-type; supramolecule.

1 Introduction

The continuous interest in exploring supramolecular assemblies that exhibit predictable functionality on the nanoscale is one of the great challenges in chemistry and materials science. One of the promising approaches in this field is choosing kinetically stable inorganic or organic moieties as secondary building blocks and their assembly into the designed structures [1–4]. In this respect, polyoxometalates (POMs) as a unique class of metal-oxo compounds, with a range of diverse compositions and considerable structural versatility, constitute one of the largest branches of inorganic precursors [5–7].

Up to now, researchers have devoted great efforts to the decoration of POMs with different organic components and a series of novel POM-based inorganic–organic hybrid compounds with a vast range of structures and properties have been obtained [8–11]. A recent advance in this field has focused on the construction of sandwich-type POM heterostructures [12–14]. However, compared with the rich information on heteropolytungstates, POM structures $([(XW_9)_2]^{n-}/[(X_2W_9)_{15}]^{n-}$, X = P, Si, Ge, As), supramolecular architectures based on heteropolymolybdate (HPM) building blocks remain largely unexplored. Possible reasons are: (1) the lability of the structures of lacunary heteropolymolybates, which can only maintain their framework in a stable system with subtle adjustments of reaction conditions. Additional ingredients can dramatically change the precursor's architectures [15, 16]; (2) the majority of HPM-based transition-metal-substituted polyoxometalates (TMSPs) were fabricated by in situ hydrothermal methods where crystalline products are hard to change to a desired structure [17–19]. Thus, choosing a suitable HPM-based sandwich-type precursor is a challenging issue for this research field. In a recent study, we found that $[M_2(AsMo_7O_{27})_2]^{12-}$ (abbreviation: $\{M_2As_2Mo_{14}\}$, M = Cr, Cu, Fe) polyoxoanions can serve as an ideal class of HPM precursors to construct new types of HPM-hybrid materials [20], not only because $\{M_2As_2Mo_{14}\}$ is a rare class of conventionally synthesized sandwiched HPMs, but also because our parallel experiments have shown that $\{M_2As_2Mo_{14}\}$ species are a kind of relatively stable HPMs, and therefore partial changes of the experimental conditions do not lead to a change of the framework.

***Corresponding authors: Xisong Miao,** Medical School, Kunming University, Yunnan, Kunming 65200, P.R. China, Fax: +86-871-65098476, E-mail: xsmiaokm@163.com; and **Hongping Ju,** Medical School, Kunming University, Yunnan, Kunming 65200, P.R. China, E-mail: jhpkmu@163.com
Qiong Wu, Jing Lu and Qingyan Zhou: Department of Chemical Science and Technology, Kunming University, Yunnan, Kunming 65200, P.R. China
Hai Wang: Key Laboratory of Yunnan Provincial Higher Education Institutions for Organic Optoelectronic Materials and Devices, Kunming University, Yunnan, Kunming 65200, P.R. China
Jun Li: Medical School, Kunming University, Yunnan, Kunming 65200, P.R. China
Yongmei Wu: School of International Cultures and Education, Yunnan University of Finance and Economics, Yunnan, Kunming 650221, P.R. China

Very recent studies revealed that further functionalization of sandwich-type POM moieties with organic molecules can enhance their activity against tumor cells. For example, in 2013, Zhou and Yang found that imidazole-modified trilacunary Keggin-type tungstobismuthates can inhibit cell proliferation and induce apoptosis in SGC-7901 cells [21]; in 2014, Wang et al. found that 1,2-diaminoethane-modified vanadium-substituted heteropolyoxoniobates exhibit remarkable activity against human gastric cancer SGC-7901, SC-1680, and MG-63 cells [22]. However, up to the present, the research on the antitumor effect toward cancer cells of sandwich-type HPM hybrid structures remains unexplored.

Based on the aforementioned considerations, we chose $[Fe_2(AsMo_7O_{27})_2]^{12-}$ as a precursor and tried to use organic cations to link these building blocks into new extended heterostructures. Herein, we report the new supramolecular compound $[Fe_2(AsMo_7O_{27})_2](H_2en)_2(NH_4)_8{\cdot}6H_2O$ (**1**). To the best of our knowledge, compound **1** represents the first example of a POM-based sandwich-type hybrid constructed from hexalacunary HPM building blocks. The magnetic properties and antitumor activities of **1** have also been studied.

2 Experimental section

All chemicals were purchased and used without further purification. The starting materials for the high-lacunary sandwiched POM building block $[Fe_2(AsMo_7O_{27})_2]^{12-}$ were synthesized according to the literature and characterized by IR spectra [20]. Elemental analyses (C, H, and N) were carried out on a Perkin-Elmer 240C instrument. Mo, Fe, and As were analyzed on a PLASMA-SPEC (I) ICP atomic emission spectrometer. TG analyses were performed on a Perkin-Elmer TGA7 instrument in flowing N_2 with a heating rate of 10°C·min^{-1}. The magnetic susceptibility measurements were carried out with the use of a Quantum Design SQUID magnetometer MPMS-XL. Measurements were performed on a polycrystalline sample of 29.39 mg.

HepG-2 cells (uterine cervical cancer cells) were purchased from the Shanghai Institute for Biological Science, Chinese Academy of Science (Shanghai, China) and were supplemented with 1 mM glutamine and 10% (*v*/*v*) fetal calf serum. Cell cultures were grown to confluence and maintained in a humidified atmosphere at 37°C and 5% CO_2. All cell lines were incubated with fetal bovine serum-free medium for 24 h prior to the experiments with the HPM (compound **1** and the precursor $\{Fe_2As_2Mo_{14}\}$). The compounds were added to a final concentration in the range of 1–100 μM. The antitumor activity of compound **1** and its parent anion on HepG-2 cells was tested by the 3-[4,5-dimethylthiazol-2-yl]-2,5-diphenyl tetrazoliumbromide (MTT) experiment.

2.1 Synthesis of 1

$(NH_4)_{12}[Fe_2(AsMo_7O_{27})_2]{\cdot}12H_2O$ (0.29 g, 0.1 mmol) was dissolved in 20 mL distilled water and stirred for 10 min. Then, 0.013 mL (0.2 mmol) ethylenediamine dissolved in 10 mL 0.02 M hydrochloric acid was added dropwise within 10 min. The mixture was kept stirring for 1 h at room temperature. The resulting reaction mixture was further refluxed for 3 h, cooled to room temperature, and filtered. Sealed with a parafilm with a few of tiny pores, a flask was kept for slow evaporation at room temperature. After 1 week, yellow block crystals were obtained (yield 35% based on Mo). – IR spectrum: see Fig. S3 (Supplementary Information available online). – Anal. for **1**: Calcd. C 1.48, H 1.67, Mo 41.41, Fe 3.44; found C 1.43, H 1.52, Mo 41.12, Fe 3.19%. TG analysis indicated that there are about six interstitial water molecules in crystals of **1** (Fig. S4; Supplementary Information).

2.2 X-ray structure determination

The intensity data of **1** were collected at 296(2) K on a Bruker D8 SMART APEX II CCD diffractometer with kappa geometry and MoK_α radiation (λ = 0.71073 Å). Suitable crystals were mounted in a thin glass capillary and transferred to the goniometer. A multi-scan absorption correction was applied. Data integration was performed using SAINT [23]. Routine Lorentz and polarization corrections were applied. Multi-scan absorption corrections were performed using SADABS [24]. Molybdenum, iron, and arsenic atoms were located by Direct Methods, and successive Fourier syntheses revealed the remaining atoms. Refinements were achieved by full-matrix least squares on F^2 using the SHELXTL crystallographic software package [25–27]. In the final refinement, all the non-H atoms were anisotropically refined. H atoms on the C and N atoms of ethylenediammonium cations were fixed on the calculated positions. The H atoms on the water molecules could not be located from the difference Fourier maps and were directly included in the final molecular formula. The NH_4^+ cations could not be precisely found from the difference Fourier maps. Therefore, the ammonium ions were also modeled as oxygen atoms. The routine SQUEEZE in PLATON [28] was used to further estimate the number of solvate water molecules and remove their electron

densities from the crystal structure. The elemental analysis and the charge balance confirmed their presence. The highest residual peak and the deepest hole are 2.61 and –1.51 e Å^{-3}, respectively. The detailed crystal data and structure refinement are given in Table 1. Bond lengths and angles around the As, Mo, and Fe centers are listed in the Supplementary Information (Tables S1 and S2).

CCDC 1057001 contains the supplementary crystallographic data for this paper. These data can be obtained free of charge from The Cambridge Crystallographic Data Centre *via* www.ccdc.cam.ac.uk/data_request/cif.

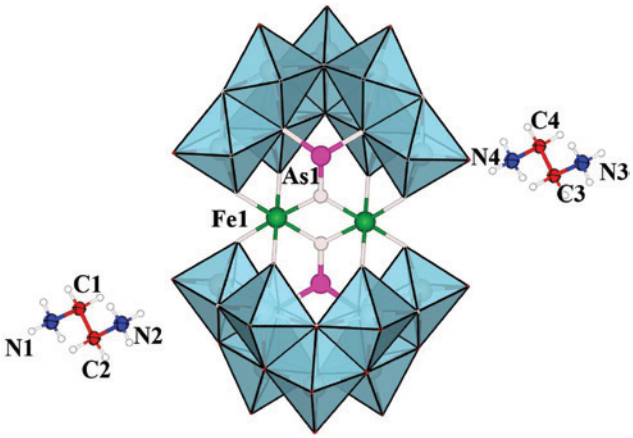

Fig. 1: Combined polyhedral and ball and stick representation of the polyoxoanion of $[Fe_2(AsMo_7O_{27})_2](H_2en)_2(NH_4)_8{\cdot}6H_2O$ (**1**). Mo blue octahedra, Fe green, As purple, O in polyanion: white; C blue. Lattice water molecules and ammonium cations are omitted for clarity.

3 Results and discussion

3.1 Description of the crystal structure

Single crystal X-ray diffraction analysis has shown that the basic structural unit of **1** contains a polyoxoanion $[Fe_2(AsMo_7O_{27})_2]^{12-}$, two ethylenediammonium cations, eight ammonium cations, and six water molecules (Fig. 1). The structural feature of $[Fe_2(AsMo_7O_{27})_2]^{12-}$ is similar to that of a previously report one [20]. Two $AsMo_7O_{27}^{9-}$ (abbreviated $\{AsMo_7\}$) units are fused together by two center Fe^{III} ions. The $\{AsMo_7\}$ unit can be deduced from hexalacunary derivatives of mono-$\{MoO_6\}$ capped α-Keggin anions $AsMo_{12}O_{40}^{3-}$ that lost six edge-sharing $\{MoO_6\}$ octahedra exposing five nucleophilic oxygen atoms. The $\{AsMo_7\}$ unit can be viewed as a multi-dentate ligand which can provide five coordination sites to chelate metal ions. The As and Mo atoms in the $\{AsMo_7\}$ unit exhibit a tri- and octahedral coordination geometry, respectively. The bond lengths As–O and the bond angles O–As–O are in the ranges of 1.761(6)–1.825(7) Å and 99.2(3)–101.4(3)°, respectively. The bond lengths Mo–O and bond angles O–Mo–O vary in the ranges 1.692(8)–2.435(7) Å and 70.1(2)–171.8(4)°, respectively (see Table S1). Both Fe^{III} ions sited in the central belt exhibit a hexa-coordinated environment and are bridged by two μ_3-O atoms derived from $\{AsO_3\}$ units. The bond lengths Fe–O and the bond angles O–Fe–O are in the ranges of 1.966(7)–2.039(7) Å and 79.5(3)–179.5(3)°, respectively. All of these bond lengths and bond angles are within the normal ranges observed in other POM complexes [29, 30].

As an interesting feature of **1**, ethylenediammonium cations (H_2en^{2+}) stabilize the $[Fe_2(AsMo_7O_{27})_2]^{12-}$ anions, as is shown in Fig. 2. The counterions H_2en^{2+} reside in the interspace of adjacent anionic units affording the first example of a hexalacunary sandwich-type supramolecular hybrid. The H_2en^{2+} cations act as donors for the neighboring anions $[Fe_2(AsMo_7O_{27})_2]^{12-}$ in N–H···O hydrogen bonds (see Table 2) and form a multiple circular hydrogen bonding environment (see Fig. 2). The $[Fe_2(AsMo_7O_{27})_2]^{12-}$ units can be abstracted as an eight-connected node that

Table 1: Crystal data and numbers pertinent to data collection and structure refinement of **1**.

Empirical formula	$C_4H_{54}As_2Fe_2Mo_{14}N_{24}O_{75}$
Formula weight M_r	3313.8
Temperature (K)	293(2)
Wavelength (Å)	0.71073
Crystal system	Triclinic
Space group	$P\bar{1}$
a (Å)	11.9794(13)
b (Å)	17.674(2)
c (Å)	19.019(2)
α (°)	63.031(2)
β (°)	87.797(2)
γ (°)	86.113(2)
Volume (Å^3)	3580.5(7)
Z	2
Calculated density (g cm^{-3})	2.60
Absorption coefficient (mm^{-1})	3.8
F(000), e	2628
θ range for data collection	1.29–27.71°
Limiting indices hkl	±15, ±23, –13→24
Reflections collected/unique/R_{int}	23 139/16 285/0.050
Completeness to θ = 25.00 (%)	97.0
Absorption correction	Semi-empirical from equivalents
Data/restraints/ref. param.	16 285/0/803
Goodness-of-fit on F^2	0.876
Final $R1/wR2$ [$I > 2\sigma(I)$]	0.0589/0.1399
$R1/wR2$ (all data)	0.1191/0.1590
Largest diff. peak/hole (e Å^{-3})	2.61/–1.51

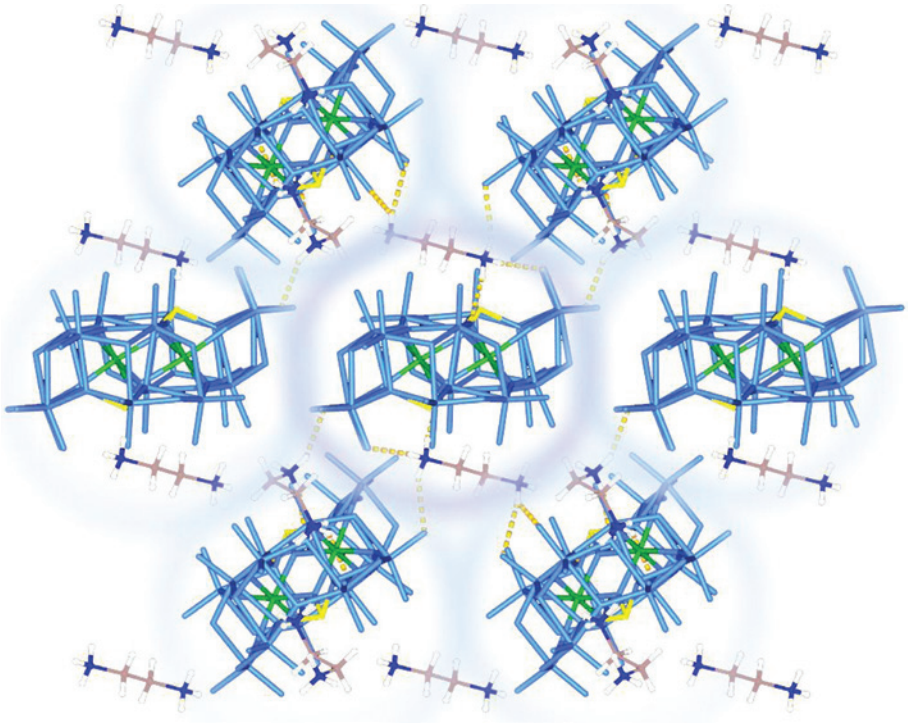

Fig. 2: Packing arrangement of compound **1** on the [100] plane, exhibiting the multiple circular hydrogen bond environment between $[Fe_2(AsMo_7O_{27})_2]^{12-}$ polyoxoanions and H_2en^{2+} cations. Mo blue octahedra, Fe green, As purple, O in polyanion: blue stick; O in ethylenediammonium red, C blue. Lattice water molecules and ammonium cations are omitted for clarity.

Table 2: Hydrogen-bond parameters (Å, °) for **1**.

D–H···A	D–H	H···A	D···A	D–H···A
N(1)–H(1A)···O(38)	0.89	2.06	2.918(15)	160
N(1)–H(1B)···O(43)	0.89	2.26	3.001(13)	140
N(1)–H(1C)···O(15)	0.89	1.99	2.848(13)	162
N(2)–H(2B)···O(29)	0.89	2.26	3.019(15)	143
N(2)–H(2B)···O(31)	0.89	2.35	2.948(13)	124
N(3)–H(3B)···O(6)	0.89	2.17	3.034(14)	163
N(3)–H(3C)···O(22)	0.89	2.08	2.905(14)	155
N(4)–H(4A)···O(26)	0.89	2.51	3.152(15)	130
N(4)–H(4A)···O(36)	0.89	2.15	2.904(14)	142
N(4)–H(4B)···O(51)	0.89	2.54	2.861(14)	102
N(4)–H(4C)···O(51)	0.89	2.35	2.943(15)	124

links with eight H_2en^{2+} cations. The H_2en^{2+} linker can be viewed as a two-connected node. Thus, the open framework of **1** can be abstracted into a 2D (8,2)-connected net supramolecular framework (see Figs. S1 and S2; Supplementary Information).

3.2 Magnetic properties

The DC measurements of **1** were performed on a powdered sample. Since all the As and Mo atoms in **1** are

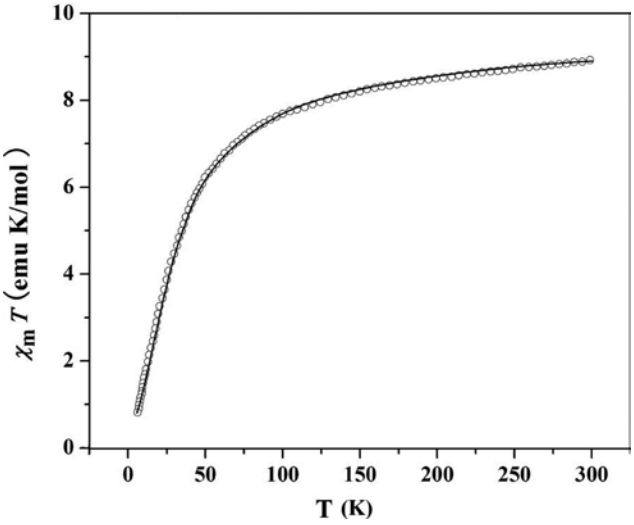

Fig. 3: Temperature dependence of the $\chi_m T$ product for **1**. The solid line is the fitting line.

diamagnetic, the magnetic behavior originates from the Fe^{III} ions. As Fig. 3 shows, the $\chi_m T$ value at room temperature is 8.91 $cm^3\ mol^{-1}\ K$, which is slightly higher than the expected value of 8.75 $cm^3\ mol^{-1}\ K$ for two spin-only uncoupled Fe(III) ($S = 5/2$, $g = 2$ for each Fe(III) ion). As the temperature was lowered, the $\chi_m T$ value remained

constant to below 50 K, and then diminished monotonically reaching to 0.33 $cm^3\ mol^{-1}$ K at 2.0 K. The behavior indicates the presence of significant antiferromagnetic interaction between two Fe^{III} ions.

Considering the long interdimer distance of **1**, the direct magnetic coupling interactions can be neglected. The susceptibility data were simulated by the isotropic exchange Hamiltonian with $H = -JS_1S_2$. The analytical expression of the susceptibility derived from this model was reported by Xue et al. [31]. The best fitting results between the calculated and experimental data were found with $J = -2.2\ cm^{-1}$ and $g = 1.99$. The negative J value indicates strong antiferromagnetic Fe–Fe interaction in **1**, the result being similar to that of a previous work [31].

3.3 Antitumor activity

The MTT method was introduced to evaluate the antitumor effect of the title compound and its precursor $(NH_4)_{12}[Fe_2(AsMo_7O_{27})_2]\cdot 12H_2O$ for HepG-2 cells in vitro. The inhibitory effects and effective cell 50% lethal concentration (IC_{50}) are given in Table 3. Both compound **1** and its precursor exhibit antitumor activities for HepG-2 cells in a dose dependent manner with the concentrations of 1–100 μM. The inhibitory effect of **1** is higher than that of the precursor. The inhibition rates of **1** on HepG-2 cells are 25%, 35%, 45%, 61%, and 74% (**1**), and those of the precursor are 22%, 32%, 40%, 59%, and 55%. The 50% lethal concentration (IC_{50}) value against HepG-2 cell lines for **1** is 221.18 μM mL^{-1}, while the value of $(NH_4)_{12}[Fe_2(AsMo_7O_{27})_2]\cdot 12H_2O$ is 313.06 μM mL^{-1}, which indicates that **1** possesses higher antitumor activities.

4 Conclusions

A new POM-based supramolecular compound has been synthesized in aqueous solution. Compound **1** represents the first example of a POM-based sandwich-type hybrid constructed from hexalacunary HPM building blocks. Further work is now in progress to introduce other POM precursors to act as inorganic building block for new types of supramolecular architectures.

Table 3: Antitumor activities of compound **1** in vitro.

Dose (μM mL^{-1})	Inhibitory effect (%)	
	1	**Precursor**
5	2	2
10	7	5
25	10	8
50	24	21
100	29	23
IC_{50} (μg mL^{-1})	220	310

5 Supplementary information

Additional bond lengths and angles, views of the hydrogen-bonding topology, IR spectrum as well as the thermogravimetric analysis curve of **1** are given as Supplementary Information available online (http://dx.doi.org/10.1515/znb-2015-0202).

Acknowledgments: This work was supported by Science and Technology Bureau of Kunming projects (No. 2015-1-S-00877; 2015-1-S-02733; 2016-1-S-02471), National Nature Science Foundation of China (No. 61166007, No. 11564023, and No. 21201090), Candidates of the Young and Middle Aged Academic Leaders of Yunnan Province and program for IRTSTYN, Applied Basic Research Programs of Science and Technology Commission Foundation of Yunnan Province (2012FD045).

References

[1] L. C. Palmer, S. I. Stupp, *Acc. Chem. Res.* **2008**, *41*, 1674.
[2] S. L. Tait, *ACS Nano* **2008**, *2*, 617.
[3] B. Moulton, M. J. Zaworotko, *Chem. Rev.* **2001**, *101*, 1629.
[4] S. C. Glotzer, M. J. Solomon, *Nat. Mater.* **2007**, *6*, 557.
[5] M.-P. Santoni, G. S. Hanan, B. Hasenknopf, *Coord. Chem. Rev.* **2014**, *281*, 64.
[6] S. Omwoma, W. Chen, R. Tsunashima, Y.-F. Song, *Coord. Chem. Rev.* **2014**, *258–259*, 58.
[7] D. Y. Du, J. S. Qin, S. L. Li, Z. M. Su, Y. Q. Lan, *Chem. Soc. Rev.* **2014**, *43*, 4615.
[8] M. Zhao, S. Ou, C.-D. Wu, *Acc. Chem. Res.* **2014**, *47*, 1199.
[9] E. L. Zhou, C. Qin, P. Huang, X. L. Wang, W. C. Chen, K. Z. Shao, Z. M. Su, *Chem. Eur. J.* **2015**, *21*, 11894.
[10] X. L. Hao, Y. Y. Ma, H. Y. Zang, Y. H. Wang, Y. G. Li, E. B. Wang, *Chem. Eur. J.* **2015**, *21*, 3778.
[11] X. Wang, L. Chen, G. Liu, J. Luan, J. Cao, C. Gong, Z. Chang, *Inorg. Chem. Commun.* **2015**, *53*, 64.
[12] B. Artetxe, S. Reinoso, L. San Felices, L. Lezama, A. Pache, C. Vicent, J. M. Gutiérrez-Zorrilla, *Inorg. Chem.* **2015**, *54*, 409.
[13] H.-Y. Zhao, J.-W. Zhao, B.-F. Yang, H. He, G.-Y. Yang, *Cryst. Growth Des.* **2013**, *13*, 5169.
[14] C.-H. Zhang, Y.-G. Chen, S.-X. Liu, *Inorg. Chem. Commun.* **2013**, *29*, 45.
[15] J. B. Cooper, D. M. Way, A. M. Bond, A. G. Wedd, *Inorg. Chem.* **1993**, *32*, 2416.
[16] T. Fukumoto, K. Murata, S. Ikeda, *Anal. Chem.* **1984**, *56*, 929.

[17] Q. Wu, Q. Han, L. Chen, P. Ma, J. Niu, *Z. Naturforsch.* **2010**, *65b*, 163.
[18] K. J. Mispa, P. Subramaniam, R. Murugesan, *Int. J. Nanosci.* **2014**, *13*, 1450002.
[19] H. Zhang, K. Yu, S. Gao, C.-M. Wang, C.-X. Wang, H.-Y. Wang, B.-B. Zhou, *Cryst. Eng. Comm.* **2014**, *16*, 8449.
[20] L. Li, Q. Shen, G. Xue, H. Xu, H. Hu, F. Feng, J. Wang, *Dalton Trans.* **2008**, *42*, 5698.
[21] L. Wang, B.-B. Zhou, K. Yu, Z.-H. Su, S. Gao, L.-L. Chu, J.-R. Liu, G.-Y. Yang, *Inorg. Chem.* **2013**, *52*, 5119.
[22] J.-Q. Shen, Q. Wu, Y. Zhang, Z.-M. Zhang, Y.-G. Li, Y. Lu, E.-B. Wang, *Chem.Eur. J.* **2014**, *20*, 2840.
[23] Smart, Saint, Area Detector Control and Integration Software, Bruker Analytical X-ray Instruments Inc., Madison, WI (USA) **1998**.
[24] G. M. Sheldrick, Sadabs, Program for Empirical Absorption Correction of Area Detector Data, University of Göttingen, Göttingen (Germany) **2002**.
[25] G. M. Sheldrick, Shelxs/l-97, Programs for Crystal Structure Determination, University of Göttingen, Göttingen (Germany) **1997**.
[26] G. M. Sheldrick, Shelxtl, Bruker Analytical X-ray Instruments Inc., Madison, WI (USA) **2001**.
[27] G. M. Sheldrick, *Acta Crystallogr.* **2008**, *A64*, 112.
[28] A. L. Spek, *Acta Crystallogr.* **2009**, *D65*, 148.
[29] A. Wutkowski, N. Evers, W. Bensch, *Z. Anorg. Allg. Chem.* **2011**, *637*, 2205.
[30] A. H. Ismail, B. S. Bassil, I. Römer, N. C. Redeker, U. Kortz, *Z. Naturforsch.* **2010**, *65b*, 383.
[31] H. Xu, L. Li, B. Liu, G. Xue, H. Hu, F. Fu, J. Wang, *Inorg. Chem.* **2009**, *48*, 10275.

Supplemental Material: The online version of this article (DOI: 10.1515/znb-2015-0202) offers supplementary material, available to authorized users.